

Deconstructed Generation-Based Zero-Shot Model

Dubing Chen¹, Yuming Shen², Haofeng Zhang¹, Philip H.S. Torr²

¹ Nanjing University of Science and Technology

² University of Oxford

{db.chen, zhanghf}@njust.edu.cn, ymcidence@gmail.com, philip.torr@eng.ox.ac.uk

Abstract

Generation-based methods have captured most of the recent attention in Zero-Shot Learning research. In this paper, we attempt to deconstruct the generator-classifier framework to guide its improvement and extension. We begin by analyzing the generator-learned instance-level distribution by alternating it with a Gaussian distribution. Then we reveal the roles of the class-level distribution and the instance-level distribution learned by the generator in classifier training by decomposing the classifier gradients. We finally conclude with the guidelines for improving the generator-classifier framework from the deconstruction of the generator and the classifier, *i.e.*, (i) The key for the ZSL generator is attribute generalization; and (ii) classifier learning emphasizes mitigating the impact of pseudo unseen samples on decision boundaries between seen classes during training, and reducing the seen-unseen bias. We propose a simple method based on the guidelines. Without complex designs, the proposed method outperforms the state of the art on four public ZSL datasets, which demonstrates the validity of the proposed guidelines. The proposed method is still effective when replacing the generative model with an attribute-to-visual center single mapping model, demonstrating its strong transferability. Codes will be public upon acceptance.

1 Introduction

With the enormous expansion of picture classes, there is a growing requirement for computer vision systems to recognize images from previously unseen classes, a challenge known as Zero-Shot Learning (ZSL) (Palatucci et al. 2009). In general, ZSL seeks to recognize unseen data by exploiting correlations between seen and unseen data. This relation mining is based on prior semantic knowledge, which is manually annotated (Lampert, Nickisch, and Harmeling 2009) or captured by word-to-vector (Mikolov et al. 2013a). Through the semantic descriptors, ZSL allows information transfer from seen to unseen domains. Recently, more researchers have paid attention to the more realistic GZSL settings, whose target decision domain contains additional seen classes compared to ZSL.

Mainstream ZSL research in recent years has utilized generative models to complement the information of unseen classes. A major hypothesis of generation-based ZSL methods is that the generated instance-level unseen distribution

fits the real unseen distribution. With the generated pseudo unseen instances, these methods enable training of the classifier covering unseen classes and yield better discrimination of unseen classes than their counterparts. Despite their success in GZSL performance, they have been facing several challenges in future extension or development, including: (i) The underlying reasons behind the effect of the generation-based approaches are still underexplored. Although some research has shown that the improved discrimination (Wu et al. 2020) or diversity (Liu et al. 2021a) of the generated samples aid in better GZSL performance, there is no theoretical or empirical evidence relevant to these performance gains. (ii) The need to train a generative model introduces additional computational and comprehensive complexity. In most generation-based methods, the training of the generative model occupies the main time complexity.

In this paper, we take a step forward to find guidance for improving the generator-classifier ZSL framework. We conduct both an empirical and a theoretical investigation to uncover, understand, and extend generation-based ZSL methods. We begin by measuring how instance-level generated unseen distributions affect the ZSL performance (Sec. 3), which indicates that the generated instance-level unseen distribution is replaceable. Then we study the role of pseudo unseen classes in classifier training from the perspective of gradients (Sec. 3.1). The whole deconstructed study points to the core improvement direction for the generator-classifier framework. First, the key for the ZSL generator is attribute generalization. That is, we should focus on generalizing the attribute-conditioned image distribution learned from the seen data to unseen classes. Second, classifier learning is an independent task to learn from partially biased data. We summarize two principles for this task, *i.e.*, mitigating the impact of pseudo unseen samples on decision boundaries between seen classes during training, and reducing the seen-unseen bias.

We finally propose a single baseline based on the idea of construction. With lower implementation complexity, our method surpasses the performance of existing methods. We also replace the generative model with a one-to-one mapping net from attributes to the class center. This without-generator method retains most of the performance. This attempt is a step towards simplifying or extending the generator-classifier framework. Our main contributions in-

clude:

- We deconstruct the behaviour of the generator and the classifier. With empirically and theoretically analysis, we expose the core of generator and classifier learning.
- From the deconstruction idea, we provide a guideline for optimizing the generator-classifier ZSL framework, based on which we derive a simple method.
- Without a complicated design of the framework, the proposed method achieves SotAs on four popular ZSL benchmark datasets. Our method can also be transferred to other generative methods, even a single attribute-vision center mapping net, which shows a step forward in simplifying the generator-classifier framework.

2 Related Work

Zero-Shot Learning (ZSL) (Lampert, Nickisch, and Harmeling 2009; Farhadi et al. 2009) has been extensively studied in recent years, which requires knowledge transfer with the class-level edge information, *e.g.*, human-defined attributes (Farhadi et al. 2009; Parikh and Grauman 2011; Akata et al. 2015) and word vectors (Mikolov et al. 2013a,b). Traditional ZSL models (Akata et al. 2013; Frome et al. 2013) typically project the attribute and the visual feature to a common space. Lampert, Nickisch, and Harmeling (2013); Frome et al. (2013); Elhoseiny, Saleh, and Elgammal (2013) choose the attribute space as the common space. Some research afterward (Zhang, Xiang, and Gong 2017; Li, Min, and Fu 2019; Skorokhodov and Elhoseiny 2021) also embed attributes to visual space, or embed attributes and visual features to another space (Akata et al. 2015; Zhang and Saligrama 2015). These methods achieve good performance in the classic ZSL setting but meet a **seen-unseen bias problem** (*i.e.*, prediction results are biased towards seen classes) in **Generalized Zero-Shot Learning (GZSL)** (Chao et al. 2016; Xian, Schiele, and Akata 2017) which emphasizes seen-unseen discrimination.

Driven by the new technology in deep learning, some research enables deeper attribute-visual association with attribute attention (Zhu et al. 2019; Huynh and Elhamifar 2020; Xu et al. 2020; Liu et al. 2021c; Wang et al. 2021). Other methods introduce the out-of-distribution discrimination (Atzmon and Chechik 2019; Min et al. 2020; Chou, Lin, and Liu 2021), which decomposes the GZSL task into seen-unseen discrimination and inter-seen (or -unseen) discrimination. The most successful methods in GZSL build on the recent advent of generative models (Goodfellow et al. 2014; Kingma and Welling 2013), which have dominated recent ZSL research. The **generation-based methods** (Xian et al. 2018, 2019; Chen et al. 2022a) construct pseudo unseen samples to constrain the decision boundary, which form a better seen-unseen discrimination than their counterparts.

A large amount of research aims at improving the generation-based framework. (Xian et al. 2019; Shen et al. 2020) focus their attention on new generative frameworks. (Verma, Brahma, and Rai 2020) explores the training method. These methods do not make full use of the prior information in the ZSL setting but seek breakthroughs from

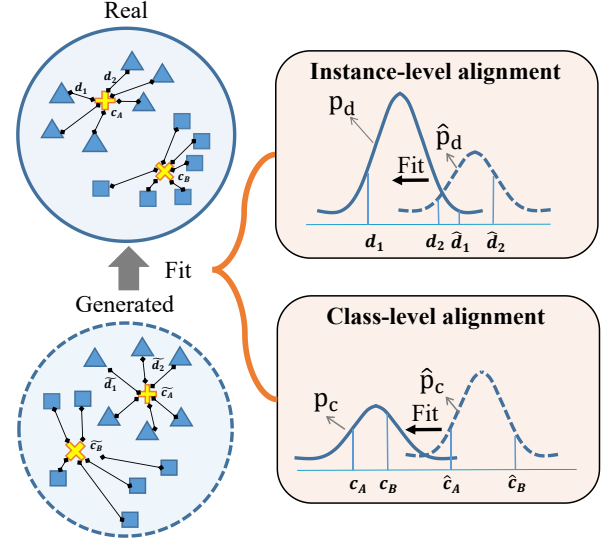


Figure 1: Illustration of the generator-learned instance-level distribution and the class-level distribution.

other fields. (Narayan et al. 2020) design a recurrent structure that utilizes the intermediate layers of the visual-to-attribute mapping network for a second generation. (Han, Fu, and Yang 2020; Han et al. 2021; Chen et al. 2021a,c; Kong et al. 2022) propose to transform the visual feature into an attribute-dependent space, the pseudo unseen samples generated in which contain less seen class bias information. The above-mentioned methods usually adopt complex strategies, which trade large time consumption for performance. In this paper, we explore the nature of the generation-based framework, surpassing current SotAs without complex design.

3 Generation-Based ZSL: A Deconstruction

Assume there are two disjoint class label sets \mathcal{Y}^s and \mathcal{Y}^u ($\mathcal{Y} = \mathcal{Y}^s \cup \mathcal{Y}^u$), ZSL aims at recognizing samples belong to \mathcal{Y}^u while only access to samples with the labels in \mathcal{Y}^s during training. Denote $\mathcal{X} \subseteq \mathbb{R}^{d_x}$ and $\mathcal{A} \subseteq \mathbb{R}^{d_a}$ as visual space and attribute space, respectively, where d_x and d_a are dimensions of these two spaces. Then $\mathbf{x} \in \mathcal{X}$ and $\mathbf{a} \in \mathcal{A}$ represent the feature instances and their corresponding attributes (represented as column vectors). Given the training set $\mathcal{D}^s = \{\mathbf{x}, y, \mathbf{a}_y | \mathbf{x} \in \mathcal{X}, y \in \mathcal{Y}^s, \mathbf{a}_y \in \mathcal{A}\}$, the goal of ZSL is to learn a classifier towards the unseen classes: $f_{zsl} : \mathcal{X} \rightarrow \mathcal{Y}^u$, while GZSL aims to classify samples that either belong to seen classes or unseen classes, *i.e.*, $f_{gzsl} : \mathcal{X} \rightarrow \mathcal{Y}$. We mainly discuss the challenges in the GZSL setting in this work.

In this paper, we focus on deconstructing the generation-classifier ZSL framework by understanding the behavior of the generator and the classifier. This type of method first trains a conditional generator with the given visual-attribute pairs. Then the pseudo unseen samples are generated with the unseen class attributes, based on which the ZSL or GZSL classifier is finally trained.

Method	DIST	T_1	A^u	A^s	H	CMMD
f-CLSWGAN	GEN	69.0	57.8	71.1	63.8	0.0337
	SVG	68.2	55.3	71.7	62.5	0.0341
	LVG	69.7	62.8	76.3	68.9	0.2523
	SCG	69.5	62.8	68.5	65.5	0.0339
CE-GZSL	GEN	69.8	63.5	77.5	69.8	0.0071
	SVG	69.4	60.1	78.2	68.0	0.0099
	LVG	66.0	47.9	72.7	57.7	0.2541
	SCG	70.6	63.2	78.9	70.2	0.0071

Table 1: Zero-Shot performance and CMMD *w.r.t.* different pseudo unseen distributions (DIST). **GEN**: Generated distribution; **SVG**: Small-variance Gaussian distribution; **LVG**: Large-variance Gaussian distribution; **SCG**: Statistical-covariance Gaussian distribution.

3.1 Empirical Analysis: If the Generator Has Learned the Instance-Level Distribution?

ZSL generative models are typically considered to have learned the unseen distribution. We divide this distribution into two parts to better analyze the ZSL generator, as illustrated in Fig. 1. One is the class-level distribution, *i.e.*, different unseen attributes are mapped to fit the real inter-class distribution in visual space. The other is the instance-level distribution, *i.e.*, samples generated by the same unseen attribute can fit the real intra-class distribution. As the class-level distribution is recognized as the core of inter-class discrimination, we focus on exploring the fitness and substitutability of the generator-led intra-class distribution.

Setup. We compare the generator fitted unseen distribution to three random Gaussian distributions with different covariance: independent small variance, independent large variance, and covariance of training data. Since the distribution generated by the typical ZSL generator is usually centralized, we replace the instance-level distribution by shifting other distribution centers to the generated class centers. The fit degree of the generated unseen samples is evaluated by comparing them with different distributions on Zero-Shot performance and distribution discrepancy against real unseen distributions. The discrepancy is measured with Maximum Mean Discrepancy (MMD), which is a typical sample-based discrepancy measurement in research of domain adaptation (Long et al. 2015) and generative models (Tolstikhin et al. 2017). We calculate MMD among the test unseen data and the experimental data for each class, and their average value is

$$\text{CMMD} = \frac{1}{|\mathcal{Y}^u|} \sum_{c=1}^{|\mathcal{Y}^u|} \left\{ \frac{1}{n_c(n_c-1)} \sum_{i,j=1, i \neq j}^{n_c} [\kappa(x_i^c, x_j^c) + \kappa(\tilde{x}_i^c, \tilde{x}_j^c)] - \frac{2}{n_c^2} \sum_{i,j=1}^{n_c} \kappa(x_i^c, \tilde{x}_j^c) \right\}, \quad (1)$$

where x_i^c and \tilde{x}_i^c are samples corresponding to class c in the test unseen set and the pseudo unseen set, respectively. n_c denotes the sample number in class c , and $\kappa(\cdot, \cdot)$ is generally an arbitrary positive-definite reproducing kernel function. Note that the test data involved here is only for measur-

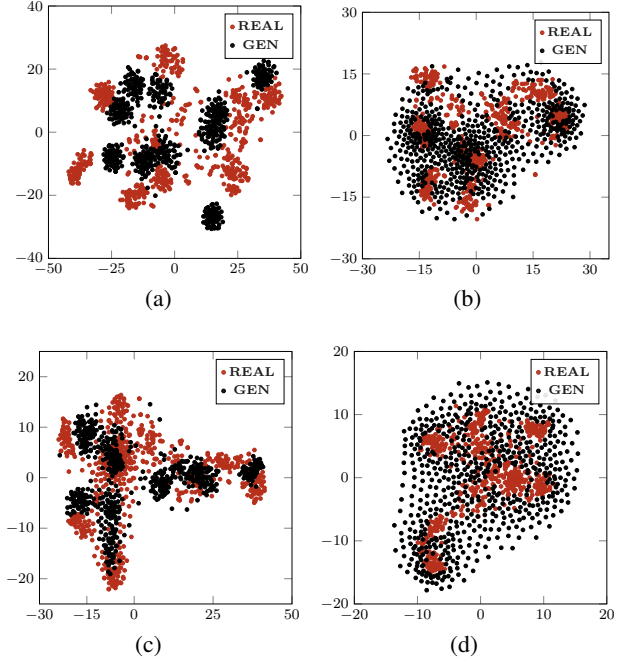


Figure 2: t-SNE comparison on different pseudo unseen distributions. **a**: Generated with f-CLSWGAN; **b**: Large-variance Gaussian distribution moved to the class center generated with f-CLSWGAN; **c**: Generated with CE-GZSL; **d**: Large-variance Gaussian distribution moved to the class center generated with CE-GZSL.

ing the distribution discrepancy and is not used in training. See the supplement for experimental details.

We conduct experiments with a distribution-insensitive method f-CLSWGAN (Xian et al. 2018) and a distribution-sensitive method CE-GZSL (Han et al. 2021) on AWA2 (Lampert, Nickisch, and Harmeling 2013). By analyzing the results in Tab. 1, we have two major conclusions: (i) In these two methods, the Gauss distribution with statistical covariance tends to exhibit similar properties to the generated distribution; and (ii) the unrealistic unseen distribution damages the performance of the distribution-sensitive method but improves the performance of the distribution-insensitive method. These two phenomena mainly motivate us to explore: (i) *Can we abandon the complex generative model and only generate the class center?* (ii) *How does the large-variance Gaussian distribution affect Zero-Shot performance?* The question (i) is experimentally verified in Sec. 5, showing that only generating class centers can achieve reasonable Zero-Shot performance. We continue to explore the role of pseudo unseen class samples in classifier training to explain the questions (i), and (ii) from the gradient perspective.

3.2 Pseudo Unseen Sample Behaviour Analysis

Suppose the linear classifier with weight parameters $\mathbf{W} \in \mathbb{R}^{|\mathcal{Y}| \times d_{\mathbf{x}}}$. With a slight abuse of notation, we subsequently use (\mathbf{x}, y) to denote both the real and generated data, and use the original notation for the normalized results. Then the

classifier is optimized with cross-entropy:

$$\begin{aligned}\mathcal{L}_{ce} &= \frac{1}{n} \sum_{c=1}^{|\mathcal{Y}|} \sum_{i=1}^{n_c} -\log p_y(\mathbf{x}_i) \\ p_y(\mathbf{x}_i) &= \frac{\exp(\langle \mathbf{W}_y, \mathbf{x}_i \rangle / \tau)}{\sum_{c=1}^{|\mathcal{Y}|} \exp(\langle \mathbf{W}_c, \mathbf{x}_i \rangle / \tau)},\end{aligned}\quad (2)$$

where $\langle \cdot, \cdot \rangle$ denotes the inner product, and the subscript c denotes the c -th row in \mathbf{W} . n is the total number of samples, n_c represents the sample amount in class c , and τ is the temperature (Hinton, Vinyals, and Dean 2015).

Proposition 3.1. *Gradients of \mathcal{L}_{ce} can be decomposed into two terms that indicate moving towards the class center and constraining the decision boundary, respectively:*

$$-\frac{\partial \mathcal{L}_{ce}}{\partial \mathbf{W}_k} = \left\{ \begin{array}{l} \frac{1}{n\tau} \sum_{i=1}^{n_k} \mathbf{x}_i \\ -\frac{1}{n\tau} \sum_{c=1}^{|\mathcal{Y}|} \sum_{j=1}^{n_c} p_k(\mathbf{x}_j) \mathbf{x}_j \end{array} \right\}, \quad (3)$$

where $p_k(\cdot)$ has an analogous definition to Eq. 2, and \mathbf{W}_k represents the classifier weight of the k th class.

The proofs of Proposition 1 is given in the supplement. Eq. 3 indicates that the primary discriminant of unseen classes is determined by the fitness of the class-level distribution. The instance-level pseudo unseen distribution controls the construction of decision boundaries.

Then why the large-variance Gaussian distribution in Sec. 3 aids in GZSL performance of f-CLSWGAN while drops the performance of CE-GZSL? Let us consider the seen-unseen bias problem, *i.e.*, the unseen class data is misidentified as the seen class. From the above-mentioned decision boundary view, a wider pseudo unseen distribution promotes wider unseen class decision boundaries, which mitigates the seen-unseen bias. As shown in Fig. 2, the large variance provides a wider pseudo unseen distribution for f-CLSWGAN that is still close to the real unseen distribution. In contrast, it does not conform to the feature distribution in CE-GZSL since this method has done a linear mapping on the original visual features. Thus, problem (i) in Sec. 3 has been solved. Based on the above view, we also derive an explanation on the common strategy of sampling a large number of pseudo unseen samples. The unseen decision boundaries are widened since an additional pseudo unseen datum \mathbf{x}^u pulls class weight \mathbf{W}^u towards the corresponding pseudo unseen distribution while pushing other class weights away.

In conclusion, we deconstruct and summarize the key points of the generator and the classifier in generation-based methods in Sec. 3, 3.1. Next, we will give specific optimization guidelines based on the above analysis.

4 Generator-Classifier Learning under the Idea of Deconstruction

4.1 Generator learning upon Attribute Generalization

Now that the instance-level is replaceable (Tab. 1), we propose to focus on optimizing the class-level distribution, which is demonstrated as the core of gradient guidance (Eq. 3). So, how to get a better class-level distribution?

We present insights from a generalization perspective. Motivated by typical supervised classification tasks where generalization means the conditional probability $q(y|\mathbf{x})$ learned from the empirical distribution $p(\mathbf{x}, y)$ fits the test set, we propose the attribute generalization:

Proposition 4.1 (Key to ZSL generator). *Attribute generalization in Zero-Shot generation is the conditional probability $p_g(\mathbf{x}|\mathbf{a})$ modeled on $p_r^s(\mathbf{x}, \mathbf{a}|\mathbf{a} \in \mathcal{A}^s)$ fitting $p_r^u(\mathbf{x}, \mathbf{a}|\mathbf{a} \in \mathcal{A}^u)$, where p_r^s and p_r^u are the real seen and unseen distributions, respectively.*

Converting a distributional learning problem into a generalization problem means that we can handle this problem directly with existing tools. Benefiting from well-established research on generalization problems in supervised classification tasks, we test some existing overfitting suppression strategies, *e.g.*, L2 regularization, the Fast Gradient Method (Goodfellow, Shlens, and Szegedy 2014) (an adversarial training method), and attribute augmentation. They all bring improvements to the original generator on ZSL performance as well as CMMD (Eq. 1) against real unseen data. See supplementary material for the results and richer experiments on attribute generalization.

4.2 Classifier learning with Partially Biased Data

Due to the absence of unseen data in ZSL setting, the generated unseen data are bound to deviate from the real distribution, as shown in Fig. 2. Therefore, learning decision boundaries that fit the true class distribution on partially deviated data is the key to classifier training. Due to the unpredictability of data bias, we need to adapt more to the deterministic distribution and reduce the adverse effects of biased distributions. Combined with the discussion in Section 3.1, we give two principles for classifier design: (i) mitigating the impact of pseudo unseen samples on decision boundaries between seen classes during training, and (ii) reducing the seen-unseen bias.

4.3 A Simple Method over the Guidelines

Over the proposed generator-classifier learning guidelines, we propose a simple method to verify its validity. We build our model on WGAN-GP (Gulrajani et al. 2017), a typical generator choice in existing ZSL researches, which contains a generator G and a discriminator D and is optimized by the following objective:

$$\begin{aligned}\mathcal{L} &= \mathbb{E}_{\mathbf{x} \sim p_r} [D(\mathbf{x}, \mathbf{a})] - \mathbb{E}_{\tilde{\mathbf{x}}} [D(\tilde{\mathbf{x}}, \mathbf{a})] \\ &\quad - \lambda_0 \mathbb{E}_{\tilde{\mathbf{x}} \sim p_{\tilde{\mathbf{x}}}} [(\nabla_{\tilde{\mathbf{x}}} \|D(\tilde{\mathbf{x}}, \mathbf{a})\|_2)^2 - 1], \quad \tilde{\mathbf{x}} = G(\mathbf{z}_0, \mathbf{a}),\end{aligned}\quad (4)$$

where p_r denotes the real distribution of \mathbf{x} , $\mathbf{z}_0 \in \mathcal{N}(\mathbf{0}, \mathbf{I})$, $\tilde{\mathbf{x}} = \alpha \mathbf{x} + (1 - \alpha) \tilde{\mathbf{x}}$ with $\alpha \sim U(0, 1)$ is for calculating the gradient penalty and λ_0 is a hyper-parameter.

We augment the attribute with Gaussian noise, to enhance the attribute generalization (Proposition 2), *i.e.*,

$$G(\mathbf{z}_0, \mathbf{a}) \rightarrow G(\mathbf{z}_0, \mathbf{a} + \mathbf{z}_1), \quad (5)$$

where $\mathbf{z}_1 \in \mathcal{N}(\mathbf{0}, \sigma \mathbf{I})$, and σ decides the standard deviation of the augmenting distribution. The reason for attribute augmentation is detailed in the supplement.

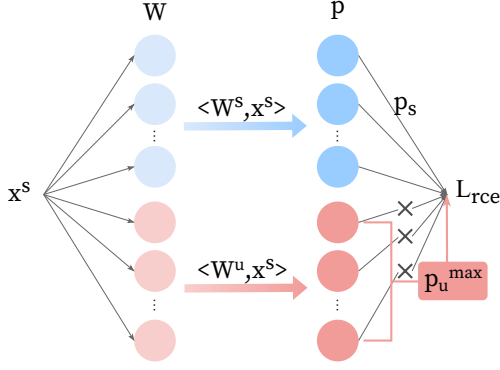


Figure 3: Illustration of the revised classifier training loss.

In the classifier training phase, guided by principle (i), we first represent the unseen class corresponding terms in loss function as the increment, *i.e.*,

$$\mathcal{L}_{ce} = \frac{1}{n} \left[\sum_{c^s=1}^{|\mathcal{Y}^s|} \sum_{i=1}^{n_{c^s}} -\log \frac{p_y(\mathbf{x}_i)}{\hat{p}^s(\mathbf{x}_i) + \lambda_1 \hat{p}^u(\mathbf{x}_i)} + \lambda_2 \sum_{c^u=1}^{|\mathcal{Y}^u|} \sum_{j=1}^{n_{c^u}} -\log p_y(\mathbf{x}_j) \right], \hat{p}^*(\mathbf{x}_i) = \sum_{c=1}^{|\mathcal{Y}^*|} p_c(\mathbf{x}_i), \quad (6)$$

where $p_c(\cdot)$ is defined in Eq. 2, 3. We introduce the parameters λ_1 and λ_2 for the generalized incremental forms, where λ_1 and λ_2 equaling to 0 means the added pseudo unseen samples do not affect the seen class decision boundaries. It indicates that principle (i) can be achieved when we choose small values of λ_1 and λ_2 .

Then we represent the gradient of \mathcal{L}_{ce} to one of the unseen class weights, \mathbf{W}_u , as

$$-\frac{\partial \mathcal{L}_{ce}}{\partial \mathbf{W}_u} = \frac{\lambda_2}{n\tau} \left(\sum_{i=1}^{n_u} \mathbf{x}_i - \sum_{c^u=1}^{|\mathcal{Y}^u|} \sum_{j=1}^{n_{c^u}} p_u(\mathbf{x}_j) \mathbf{x}_j \right) - \frac{1}{n\tau} \sum_{c^s=1}^{|\mathcal{Y}^s|} \sum_{k=1}^{n_{c^s}} \frac{\lambda_1 p_u(\mathbf{x}_k)}{\hat{p}^s(\mathbf{x}_k) + \lambda_1 \hat{p}^u(\mathbf{x}_k)} \mathbf{x}_k, \quad (7)$$

where a small λ_1 makes the seen data have little effect on the decision boundaries of unseen classes, and the value of λ_2 controls the attention of the loss function on the inter-unseen-class decision boundaries. This provides a direction to mitigate the seen-unseen bias, *i.e.*, the principle (ii).

In summary, a small λ_1 and a suitable λ_2 fit the two principles that guide the classifier design. We remove the parameter λ_2 since it provides the same optimization direction with the generation number of pseudo unseen samples. We set different λ_1 values for each unseen class according to their optimization difficulty. Empirically, we only set non-zero values for the hardest class, and only if it is greater than the true class score, as shown in Fig. 3. The revised cross-entropy is

$$\mathcal{L}_{rce} = \frac{1}{n} \sum_{c^s=1}^{|\mathcal{Y}^s|} \sum_{i=1}^{n_{c^s}} -\log \frac{p_y(\mathbf{x}_i)}{\hat{p}^s(\mathbf{x}_i) + \lambda_1 \mathbb{1}[p_m(\mathbf{x}_i) > p_y(\mathbf{x}_i)] p_m(\mathbf{x}_i)} + \sum_{c^u=1}^{|\mathcal{Y}^u|} \sum_{j=1}^{n_{c^u}} -\log p_y(\mathbf{x}_j), p_m(\mathbf{x}_i) = \max \{p_c(\mathbf{x}_i) | c \in \mathcal{Y}^u\}, \quad (8)$$

where $\mathbb{1}$ is the indicator function, which equals 1 if the condition is true, and 0 otherwise. As shown in Fig. 4 (c), (d), the classifier obtained with a suitable value of λ_1 has stronger inter-seen class discriminability and smaller seen-unseen bias. Finally, we bound the classifier weights with the attributes, following a common strategy in ZSL. We directly employ a mapping network $M(\cdot)$ to map attributes to the classification weights, *i.e.*,

$$\mathbf{W}_c = M(\mathbf{a}_c), c \in \mathcal{Y}^s \cup \mathcal{Y}^u, \quad (9)$$

which replaces the weights in Eq. 2. After training, a datum \mathbf{x} is predicted as the class corresponding to the attribute with the largest similarity to \mathbf{x} , *i.e.*,

$$\hat{y} = \arg \max_c \langle M(\mathbf{a}_c), \mathbf{x} \rangle, \quad (10)$$

5 Experiments

Benchmark Datasets. We conduct GZSL experiments on four public ZSL datasets. Animals with Attributes 2 (AWA2) (Lampert, Nickisch, and Harmeling 2013) contains 50 animal species and 85 attribute annotations, accounting 37,322 samples. Attribute Pascal and Yahoo (APY) (Farhadi et al. 2009) includes 32 classes of 15,339 samples and 64 attributes. Caltech-UCSD Birds-200-2011 (CUB) (Wah et al. 2011) consists of 11,788 samples with 200 bird species, annotated by 312 attributes. SUN Attribute (SUN) (Patterson and Hays 2012) carries 14,340 images from 717 different scenario-style with 102 attributes. We split the data into seen and unseen classes according to the common benchmark procedure in Xian, Schiele, and Akata (2017).

Representation. We conduct most experiments with the 2048-dimensional visual features extracted from the pre-trained ResNet101 (He et al. 2016) without fine-tuning on seen data, following Xian, Schiele, and Akata (2017). We also compare the GZSL performance on the fine-tuned data that we take from Chen et al. (2021c). For class representations (*i.e.*, attributes), we adopt the artificial attribute annotations that come with the datasets for AWA2, APY, and SUN, and regard the 1024-dimensional character-based CNN-RNN features (Reed et al. 2016) generated from textual descriptions as the attributes of CUB, for a fair comparison with SotAs.

Evaluation Metric. We calculate the average per-class top-1 accuracy on the unseen and seen classes respectively, denoted as A^u and A^s , then their harmonic mean H is employed as the measurement of GZSL. The classic ZSL is evaluated with per-class averaged top-1 accuracy on unseen classes (Xian, Schiele, and Akata 2017).

Implementation Details. The method proposed in 4 is implemented with three modules. The Generator G consists of a multi-layer perceptron (MLP) with two hidden layers of 4096 and 2048 dimensions. The Discriminator D contains one 4096-D hidden layer, and the mapping net M includes a 1024-D hidden layer. All the hidden layers are activated by Leaky-ReLU. We follow Xian et al. (2018) to set other hyper-parameters in WGAN-GP. In addition, we set 512 for the (mini) batch size, and adopt Adam (Kingma and Ba 2015) as the optimizer of all the nets with learning rate of 1.0×10^{-4} .

Method			Source	AWA2			CUB			SUN			APY		
				A^u	A^s	H	A^u	A^s	H	A^u	A^s	H	A^u	A^s	H
‡	TGMZ	AAAI 2021d	64.1	77.3	70.1	60.3	56.8	58.5	-	-	-	34.8	77.1	48.0	
	Chou et al.	ICLR 2021	65.1	78.9	71.3	41.4	49.7	45.2	29.9	40.2	34.3	35.1	65.5	45.7	
	SDGZSL	ICCV2021c	64.6	73.6	68.8	59.9	66.4	63.0	48.2	36.1	41.3	38.0	57.4	45.7	
	FREE	ICCV 2021a	60.4	75.4	67.1	55.7	59.9	57.7	47.4	37.2	41.7	-	-	-	
	GCM-CF	CVPR 2021	60.4	75.1	67.0	61.0	59.7	60.3	47.9	37.8	42.2	37.1	56.8	44.9	
	CE-GZSL	CVPR 2021	63.1	78.6	70.0	63.9	66.8	65.3	48.8	38.6	<u>43.1</u>	-	-	-	
	HSVA	NeurIPS 2021b	56.7	79.8	66.3	52.7	58.3	55.3	-	-	-	-	-	-	
	SE-GZSL	AAAI 2022	59.9	80.7	68.8	53.1	60.3	56.4	45.8	40.7	<u>43.1</u>	-	-	-	
	ICCE	CVPR 2022	65.3	82.3	<u>72.8</u>	67.3	65.5	66.4	-	-	-	45.2	46.3	45.7	
	DGZ	Proposed	67.4	81.0	73.6	70.1	68.3	69.2	48.6	39.4	43.5	39.2	65.1	48.9	
DGZ w/o GM	65.9		78.2	71.5	71.4	64.8	<u>68.0</u>	49.9	37.6	42.8	38.5	66.0	<u>48.6</u>		
†	TF-VAEGAN*	ECCV 2020	55.5	83.6	66.7	63.8	79.3	70.7	41.8	51.9	<u>46.3</u>	-	-	-	
	Chou et al.*	ICLR 2021	69.0	86.5	<u>76.8</u>	69.2	76.4	72.6	50.5	43.1	46.5	36.2	58.6	44.8	
	GEM-ZSL	CVPR 2021c	64.8	77.5	<u>70.6</u>	64.8	77.1	70.4	38.1	35.7	36.9	-	-	-	
	SDGZSL*	ICCV2021c	69.6	78.2	73.7	73.0	77.5	75.1	51.1	40.2	45.0	39.1	60.7	47.5	
	DPPN	NeurIPS 2021	63.1	86.8	73.1	70.2	77.1	73.5	47.9	35.8	41.0	40.0	61.2	48.4	
	TransZero	AAAI 2022b	61.3	82.3	70.2	69.3	68.3	68.8	52.6	33.4	40.8	-	-	-	
	MSDN	CVPR 2022c	62.0	74.5	67.7	68.7	67.5	68.1	52.2	34.2	41.3	-	-	-	
	DGZ*	Proposed	71.7	83.7	77.2	76.9	77.7	<u>77.3</u>	49.4	43.5	<u>46.3</u>	37.1	79.3	50.5	
	DGZ* w/o GM		67.2	85.7	75.4	77.4	78.0	77.7	50.4	39.8	44.5	38.5	67.4	<u>49.0</u>	

Table 2: GZSL performance comparison with the state-of-the-art methods on four popular benchmarks. † denotes enabling finetuning with the original image, and * represents generative methods based on the features extracted from the finetuned backbone. ‡ denotes generative methods based on the common image feature proposed in Xian, Schiele, and Akata (2017). A^u and A^s represent per-class accuracy scores (%) on seen and unseen test sets, and H is their harmonic mean. The best result is bolded, and the second-place result is underlined.

5.1 Comparison with State of the Arts

We evaluate the simple method in Sec. 4 to verify the validity of the proposed guidelines. The GZSL results are compared with SotAs in Tab. 2. It can be observed that our results on common image feature outperform SotAs in all of the four datasets. The results based on the fine-tuning feature reach the first place on the three datasets, only second to Chou, Lin, and Liu (2021) on SUN. Especially, our method does not rely on any complex designs. This simple derivation from guidance outperforms other approaches with high complexity *e.g.*, Chou, Lin, and Liu (2021) employs the out-of-distribution discrimination method, and (Han et al. 2021; Kong et al. 2022) are based on instance discrimination, which all lead to huge time cost.

We also report the results without a generative model, *i.e.*, replacing the generator with a one-to-one mapping network from attributes to visual centers. The pseudo unseen distribution is the is a Gaussian distribution with the generated class centers and statistical covariance as parameters. In this baseline, our method still achieves comparable performance with current SotAs, which demonstrates the plug-in capability of the proposed classifier learning strategy. It is also a attempt towards simplify the generator-classifier framework. More explanatory experiments can be found in the supplementary material.

5.2 Ablation Study

Baselines. We conduct an ablation study to validate the effect of each component, with following baselines: (i) We set σ to 0 in the full model. (ii) Training the classifier with the

Ablation		AWA2			CUB		
		A^u	A^s	H	A^u	A^s	H
(i)	w/o ATA	66.4	77.2	71.4	72.2	66.1	69.0
(ii)	w/o CR	39.8	89.4	55.1	58.3	70.9	64.0
(iii)	w/o M	64.0	79.4	70.9	70.7	57.8	63.6
(iv)	w/o CR&M	34.7	90.0	50.0	44.7	70.2	54.7
(v)	DIST \rightarrow SCG	67.5	78.0	72.4	68.3	67.7	68.0
(vi)	DIST \rightarrow GC+SCG	65.9	78.2	71.5	71.4	64.8	68.0
Full Model		67.4	81.0	73.6	70.1	68.3	69.2

Table 3: Ablation study results of GZSL on AWA2 and CUB. The baselines are constructed by removing some key modules. **ATA**: Attribute augmentation; **CR**: Classifier revision; **M**: Mapping net. **SCG**: Statistical-covariance Gaussian distribution. **GC**: Direct generating the class center.

vanilla cross-entropy, *i.e.*, Eq. 2. (iii) Without mapping net, *i.e.*, optimizing the randomly generated class weights. (iv) Without classifier revision and mapping net. (v) Alternating the WGAN-generated distribution with the statistical-covariance Gaussian distribution (same to Sec. 3). (vi) On the basis of (v), replacing the generative model with a class center generating net (same to Sec. 5.1).

Results. The ablation study is conducted on AWA2 and CUB datasets, of which the results are shown in Tab. 3 with the GZSL performance. **Baseline i** shows that the attribute augmentation produces fewer effects on the fine-grained dataset CUB than on the coarse-grained dataset AWA2. It is mainly because of the inherently small data bias caused by more types of attributes in the generator training of CUB (40 in AWA2 vs 150 in CUB). Meanwhile, for the same rea-

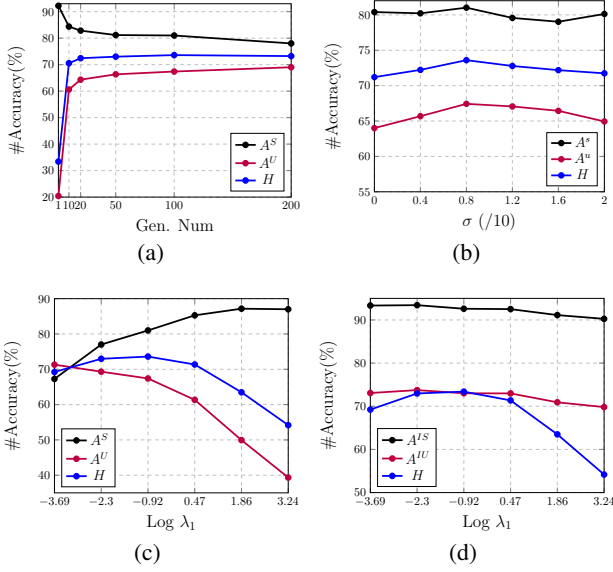


Figure 4: (a), (b), (c) GZSL effects w.r.t. the generated number for each unseen classes, σ , and λ_1 . (d) Intra-discriminability of seen and unseen classes w.r.t. λ_1 , where A^{is} and A^{iu} represent the intra- seen or unseen classes accuracy, and H is still the harmonic mean of A^s and A^u . We conduct the study on AWA2.

son, classifier revision plays a bigger role for AWA2 than for CUB (**baseline ii, iv**). As shown in **baseline iii, iv**, the ablation of the mapping network also degrades performance since it creates implicit semantic connections between classifier weights. Overall, attribute generalization enhancement brings fewer performance gains than classifier revision since its intractability. **Baseline v and vi** compare the directly generated class center and the class center by averaging the samples generated by the generative model. The class center derived from the generative model achieves better performance. It is probably because the instance-level modeling extracts more distribution information and generalizes better to unseen class attributes. More details and analysis are in the supplementary material.

5.3 Hyper-parameters

There are mainly four hyper-parameters that control the objective function, *i.e.*, σ , τ , λ_1 , and the generated number per unseen class. For τ , we follow (Skorokhodov and Elhoseiny 2021) to assign it a value of 0.04 on all datasets. Then we empirically analyze the influence of the other three parameters on AWA2. As shown in Fig. 4 (b), A^u and H have the same trend when σ varies, which demonstrates its ability to control the attribute generalization effect. A big σ leads to performance degradation because a large variance of noise intuitively makes the attribute input of the generator lose inter-class discriminability. A small λ_1 mitigates the seen-unseen bias in Fig. 4 (c). In the meantime, a suitable generated number creates the best performance, as shown in Fig. 4 (a), and the number is much smaller than the existing generation-based methods (100 vs. 2400 in (Han et al. 2021)

Method	AWA2	CUB	SUN	APY
TCN (2019)	71.2	59.5	61.5	38.9
LisGAN (2019)	-	58.8	61.7	43.1
TF-VAEGAN (2020)	72.2	64.9	66.0	-
Chou et al. (2021)	73.8	57.2	63.3	41.0
IPN (2021b)	74.4	59.6	-	42.3
CE-GZSL (2021)	70.4	77.5	63.3	-
SDGZSL (2021c)	72.1	75.5	-	45.4
DGZ	74.0	80.1	65.4	46.6

Table 4: Discriminability on unseen classes, evaluated by ZSL performance (%) (comparison with SotAs). **Note** that our classifier is obtained with targeting at GZSL.

and 4600 in (Chen et al. 2021a)). This demonstrates the joint effect of the number of generations and λ_1 we stated in Sec. 4. We also report the effect of λ_1 on the intra-seen class discriminability in Fig. 4 (d), which shows a downward trend when λ_1 increases within a certain range. We empirically generate 50 samples per unseen class in CUB, SUN, and APY, and 100 for AWA2 in the experiment. We set λ_1 to 12 for CUB and 0.4 for the other three datasets for the best results. σ is set to 0.08 on all datasets.

5.4 Discriminability on Unseen Classes

We analyze the discriminability of the trained classifier on unseen classes, which is obtained under the GZSL setting. We directly employ the ZSL accuracy as the measurement, compared with SotAs in Tab. 4. Surprisingly, although our model does not target ZSL directly, it still achieves promising ZSL performance, even comparable to SotA methods trained towards ZSL setting. We believe that there are two main reasons for the good discriminability in unseen classes. One is the improvement of attribute generalization ability, and the other is the intrinsic semantic association of classifier weights derived from attribute mapping.

6 Conclusion

In this paper, we deconstruct the generator-classifier Zero-Shot Learning framework. We analyze the role of pseudo unseen samples in classifier training by decomposing the gradient of cross-entropy. We reveal that the unseen class discrimination is mainly controlled by the generated class-level distribution. The instance-level distribution affects the extent of the decision boundary, which is empirically replaceable by a fixed distribution. We further analyze the effect of previous methods on the gradient, and conclude that they mitigate the seen-unseen bias problem. By summarizing all the analyses, we propose a design guideline for the generator-classifier framework. Specifically, we emphasize attribute generalization in generator training and regard classifier training as a independent task to learn from partially biased data. Based on these points, we propose a simple method that outperforms current SotAs in performance without a complex design, demonstrating the effectiveness of the proposed guideline. We test the transferability of the proposed classifier revision strategy and find that our method can achieve SotA even if we replace the generative model with a class center

mapping net. In the future, we will conduct closer research to simplify the generation-based method.

References

- Akata, Z.; Perronnin, F.; Harchaoui, Z.; and Schmid, C. 2013. Label-embedding for attribute-based classification. In *CVPR*, 819–826.
- Akata, Z.; Reed, S.; Walter, D.; Lee, H.; and Schiele, B. 2015. Evaluation of output embeddings for fine-grained image classification. In *CVPR*, 2927–2936.
- Atzmon, Y.; and Chechik, G. 2019. Adaptive confidence smoothing for generalized zero-shot learning. In *CVPR*, 11671–11680.
- Chao, W.-L.; Changpinyo, S.; Gong, B.; and Sha, F. 2016. An empirical study and analysis of generalized zero-shot learning for object recognition in the wild. In *ECCV*, 52–68.
- Chen, D.; Shen, Y.; Zhang, H.; and Torr, P. H. 2022a. Zero-Shot Logit Adjustment. In Raedt, L. D., ed., *IJCAI*, 813–819. International Joint Conferences on Artificial Intelligence Organization.
- Chen, S.; Hong, Z.; Liu, Y.; Xie, G.-S.; Sun, B.; Li, H.; Peng, Q.; Lu, K.; and You, X. 2022b. TransZero: Attribute-guided Transformer for Zero-Shot Learning. In *AAAI*.
- Chen, S.; Hong, Z.; Xie, G.-S.; Yang, W.; Peng, Q.; Wang, K.; Zhao, J.; and You, X. 2022c. MSDN: Mutually Semantic Distillation Network for Zero-Shot Learning. In *CVPR*, 7612–7621.
- Chen, S.; Wang, W.; Xia, B.; Peng, Q.; You, X.; Zheng, F.; and Shao, L. 2021a. FREE: Feature Refinement for Generalized Zero-Shot Learning. In *ICCV*.
- Chen, S.; Xie, G.; Liu, Y.; Peng, Q.; Sun, B.; Li, H.; You, X.; and Shao, L. 2021b. Hsva: Hierarchical semantic-visual adaptation for zero-shot learning. In *NeurIPS*.
- Chen, Z.; Luo, Y.; Qiu, R.; Huang, Z.; Li, J.; and Zhang, Z. 2021c. Semantics Disentangling for Generalized Zero-shot Learning. In *ICCV*.
- Chou, Y.-Y.; Lin, H.-T.; and Liu, T.-L. 2021. Adaptive and generative zero-shot learning. In *ICLR*.
- Elhoseiny, M.; Saleh, B.; and Elgammal, A. 2013. Write a classifier: Zero-shot learning using purely textual descriptions. In *ICCV*, 2584–2591.
- Farhadi, A.; Endres, I.; Hoiem, D.; and Forsyth, D. 2009. Describing objects by their attributes. In *CVPR*, 1778–1785.
- Frome, A.; Corrado, G.; Shlens, J.; Bengio, S.; Dean, J.; Ranzato, M.; and Mikolov, T. 2013. Devise: A deep visual-semantic embedding model. In *NeurIPS*, 2121–2129.
- Goodfellow, I.; Pouget-Abadie, J.; Mirza, M.; Xu, B.; Warde-Farley, D.; Ozair, S.; Courville, A.; and Bengio, Y. 2014. Generative adversarial nets. In *NeurIPS*.
- Goodfellow, I. J.; Shlens, J.; and Szegedy, C. 2014. Explaining and harnessing adversarial examples. arXiv:1412.6572.
- Gulrajani, I.; Ahmed, F.; Arjovsky, M.; Dumoulin, V.; and Courville, A. 2017. Improved training of wasserstein gans. In *NeurIPS*.
- Han, Z.; Fu, Z.; Chen, S.; and Yang, J. 2021. Contrastive Embedding for Generalized Zero-Shot Learning. In *CVPR*, 2371–2381.
- Han, Z.; Fu, Z.; and Yang, J. 2020. Learning the redundancy-free features for generalized zero-shot object recognition. In *CVPR*, 12865–12874.
- He, K.; Zhang, X.; Ren, S.; and Sun, J. 2016. Deep residual learning for image recognition. In *CVPR*, 770–778.
- Hinton, G.; Vinyals, O.; and Dean, J. 2015. Distilling the knowledge in a neural network. In *NeurIPS*.
- Huynh, D.; and Elhamifar, E. 2020. Fine-grained generalized zero-shot learning via dense attribute-based attention. In *CVPR*, 4483–4493.
- Jiang, H.; Wang, R.; Shan, S.; and Chen, X. 2019. Transferable contrastive network for generalized zero-shot learning. In *ICCV*, 9765–9774.
- Kim, J.; Shim, K.; and Shim, B. 2022. Semantic feature extraction for generalized zero-shot learning. In *AAAI*, 1166–1173.
- Kingma, D. P.; and Ba, J. 2015. Adam: A method for stochastic optimization. In *ICLR*.
- Kingma, D. P.; and Welling, M. 2013. Auto-encoding variational bayes. In *ICLR*.
- Kong, X.; Gao, Z.; Li, X.; Hong, M.; Liu, J.; Wang, C.; Xie, Y.; and Qu, Y. 2022. En-Compactness: Self-Distillation Embedding & Contrastive Generation for Generalized Zero-Shot Learning. In *CVPR*, 9306–9315.
- Lampert, C. H.; Nickisch, H.; and Harmeling, S. 2009. Learning to detect unseen object classes by between-class attribute transfer. In *CVPR*, 951–958.
- Lampert, C. H.; Nickisch, H.; and Harmeling, S. 2013. Attribute-based classification for zero-shot visual object categorization. *IEEE TPAMI*, 453–465.
- Li, J.; Jing, M.; Lu, K.; Ding, Z.; Zhu, L.; and Huang, Z. 2019. Leveraging the invariant side of generative zero-shot learning. In *CVPR*, 7402–7411.
- Li, K.; Min, M. R.; and Fu, Y. 2019. Rethinking zero-shot learning: A conditional visual classification perspective. In *ICCV*, 3583–3592.
- Liu, J.; Bai, H.; Zhang, H.; and Liu, L. 2021a. Near-Real Feature Generative Network for Generalized Zero-Shot Learning. In *ICME*, 1–6.
- Liu, L.; Zhou, T.; Long, G.; Jiang, J.; Dong, X.; and Zhang, C. 2021b. Isometric propagation network for generalized zero-shot learning. In *ICLR*.
- Liu, Y.; Zhou, L.; Bai, X.; Huang, Y.; Gu, L.; Zhou, J.; and Harada, T. 2021c. Goal-oriented gaze estimation for zero-shot learning. In *CVPR*, 3794–3803.
- Liu, Z.; Li, Y.; Yao, L.; Wang, X.; and Long, G. 2021d. Task aligned generative meta-learning for zero-shot learning. In *AAAI*, 8723–8731.
- Long, M.; Cao, Y.; Wang, J.; and Jordan, M. 2015. Learning transferable features with deep adaptation networks. In *ICML*, 97–105. PMLR.

- Mikolov, T.; Chen, K.; Corrado, G.; and Dean, J. 2013a. Efficient estimation of word representations in vector space. In *ICLR Work-shop Papers*.
- Mikolov, T.; Sutskever, I.; Chen, K.; Corrado, G. S.; and Dean, J. 2013b. Distributed representations of words and phrases and their compositionality. In *NeurIPS*.
- Min, S.; Yao, H.; Xie, H.; Wang, C.; Zha, Z.-J.; and Zhang, Y. 2020. Domain-aware visual bias eliminating for generalized zero-shot learning. In *CVPR*, 12664–12673.
- Narayan, S.; Gupta, A.; Khan, F. S.; Snoek, C. G.; and Shao, L. 2020. Latent embedding feedback and discriminative features for zero-shot classification. In *ECCV*, 479–495.
- Palatucci, M. M.; Pomerleau, D. A.; Hinton, G. E.; and Mitchell, T. 2009. Zero-shot learning with semantic output codes. In *NeurIPS*. Carnegie Mellon University.
- Parikh, D.; and Grauman, K. 2011. Relative attributes. In *ICCV*, 503–510. IEEE.
- Patterson, G.; and Hays, J. 2012. Sun attribute database: Discovering, annotating, and recognizing scene attributes. In *CVPR*, 2751–2758.
- Reed, S.; Akata, Z.; Lee, H.; and Schiele, B. 2016. Learning deep representations of fine-grained visual descriptions. In *CVPR*, 49–58.
- Shen, Y.; Qin, J.; Huang, L.; Liu, L.; Zhu, F.; and Shao, L. 2020. Invertible zero-shot recognition flows. In *ECCV*, 614–631.
- Skorokhodov, I.; and Elhoseiny, M. 2021. Class Normalization for (Continual)? Generalized Zero-Shot Learning. In *ICLR*.
- Tolstikhin, I.; Bousquet, O.; Gelly, S.; and Schoelkopf, B. 2017. Wasserstein auto-encoders. In *ICLR*.
- Verma, V. K.; Brahma, D.; and Rai, P. 2020. Meta-learning for generalized zero-shot learning. In *AAAI*, 6062–6069.
- Wah, C.; Branson, S.; Welinder, P.; Perona, P.; and Belongie, S. 2011. The caltech-ucsd birds-200-2011 dataset. Technical report, california institute of technology.
- Wang, C.; Min, S.; Chen, X.; Sun, X.; and Li, H. 2021. Dual Progressive Prototype Network for Generalized Zero-Shot Learning. In *NeurIPS*, 2936–2948.
- Wu, J.; Zhang, T.; Zha, Z.-J.; Luo, J.; Zhang, Y.; and Wu, F. 2020. Self-supervised domain-aware generative network for generalized zero-shot learning. In *CVPR*, 12767–12776.
- Xian, Y.; Lorenz, T.; Schiele, B.; and Akata, Z. 2018. Feature generating networks for zero-shot learning. In *CVPR*, 5542–5551.
- Xian, Y.; Schiele, B.; and Akata, Z. 2017. Zero-shot learning-the good, the bad and the ugly. In *CVPR*, 4582–4591.
- Xian, Y.; Sharma, S.; Schiele, B.; and Akata, Z. 2019. f-gan-d2: A feature generating framework for any-shot learning. In *CVPR*, 10275–10284.
- Xu, W.; Xian, Y.; Wang, J.; Schiele, B.; and Akata, Z. 2020. Attribute prototype network for zero-shot learning. In *NeurIPS*, 21969–21980.
- Yue, Z.; Wang, T.; Sun, Q.; Hua, X.-S.; and Zhang, H. 2021. Counterfactual zero-shot and open-set visual recognition. In *CVPR*, 15404–15414.
- Zhang, L.; Xiang, T.; and Gong, S. 2017. Learning a deep embedding model for zero-shot learning. In *CVPR*, 2021–2030.
- Zhang, Z.; and Saligrama, V. 2015. Zero-shot learning via semantic similarity embedding. In *ICCV*, 4166–4174.
- Zhu, Y.; Xie, J.; Tang, Z.; Peng, X.; and Elgammal, A. 2019. Semantic-guided multi-attention localization for zero-shot learning. In *NeurIPS*.